Electronic Supplementary Material (ESI) for Inorganic Chemistry Frontiers.

Nanocomposite of MoO_2 and MoC loaded on porous carbon as an efficient electrocatalyst for hydrogen evolution reaction

Cuncai Lv[a,b], *Zhipeng Huang*[a,*], *Qianpeng Yang*[a,b], *and Chi Zhang*[a,*]

[a]School of Chemical Science and Engineering, and Institute for Advanced Study, Tongji University, Shanghai, 200092, PR China.

[b]School of Materials Science and Engineering, Jiangsu University, Zhenjiang, 212013, PR China.

* Corresponding author: E-mail: zphuang@tongji.edu.cn, chizhang@tongji.edu.cn

Electronic Supplementary Information

Section 1. DFT calculations

The DFT calculations were carried out using CASTEP (Cambridge Serial Total Energy Package)[1] with a plane-wave basis set and ultrasoft pseudo-potentials.[2] The exchange correlation contribution to the total electronic energy was treated in a generalized gradient corrected (GGA) approximation (Perdew-Burke-Ernzerhoff functional).[3] A plane-wave energy cutoff of 300 eV was used for the rapid comparison of different adsorption configurations while 380 eV was used for the adsorption energy calculations. The Monkhorst-Pack (3 × 5 × 1) k-point mesh was utilized for the first Brillouin zone integrations. The structural parameters were determined using the Broyden-Fletcher-Goldfarb-Shanno (BFGS) minimization technique. The thresholds for the converged structures were as follows: energy change less than 1×10^{-5} eV atom^{-1}, the maximum residual force less than 0.02 eV Å^{-1}, the maximum displacement of atoms less than 0.001 Å, and the maximum stress less than 0.05 GPa.

The surface energy (SE) was defined as the change in energy from bulk to the surface normalized by the area of each surface. The SE can be calculated as:

$$SE = (E_{surface} - N * (E_{bulk}/n))/(2 * A)$$

where $E_{surface}$ is the energy of a surface cell, E_{bulk} is the energy of a bulk cell, N is the number of atoms in the surface cell, n is the number of atoms in the bulk cell, and A is the area of a surface.

The differential adsorption energy of H adsorption was chosen to describe the stability of hydrogen, the equation being given below:

$\Delta E_H = E(nH^*) - E((n-1)H^*) - 1/2E(H_2)$ where $E(nH^*)$ is the total energy of the model with n hydrogen atoms adsorbed on the surface, $E((n-1)H^*)$ is the total energy of the model with (n-1) hydrogen atoms adsorbed on the surface, and $E(H_2)$ is the total energy of a hydrogen molecule in the gas phase. n is 1 in our calculations.

The Gibbs free energy for hydrogen adsorption was calculated as below:

$$\Delta G_{H^*} = \Delta E_H + \Delta E_{ZPE} - T\Delta S_H$$

where ΔE_{ZPE} is the difference in zero-point energy between the adsorbed state and the gas phase and ΔS_H is the entropy difference between the adsorbed state and the gas phase. The overall corrections are taken as: [4]

$$\Delta G_{H^*} = \Delta E_H + 0.24\ eV$$

In the calculation of ΔG_{H^*}, a unit cell of MoO_2 (101) was composed of 8 atomic layers and a vacuum region with a thickness of 20 Å. A MoC (001) unit cell contained 8 atomic layers and 20 Å-thick vacuum slab. In the two unit cells, the bottom four atomic layers of were fixed, and the other atoms were allowed to relax.

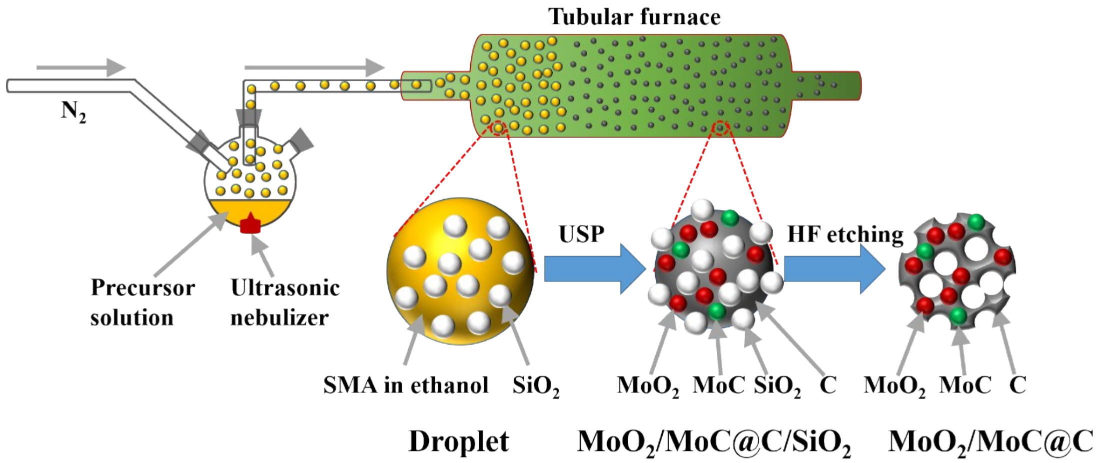

Fig. S1. The setup of synthesis of MoO_2/MoC@C.

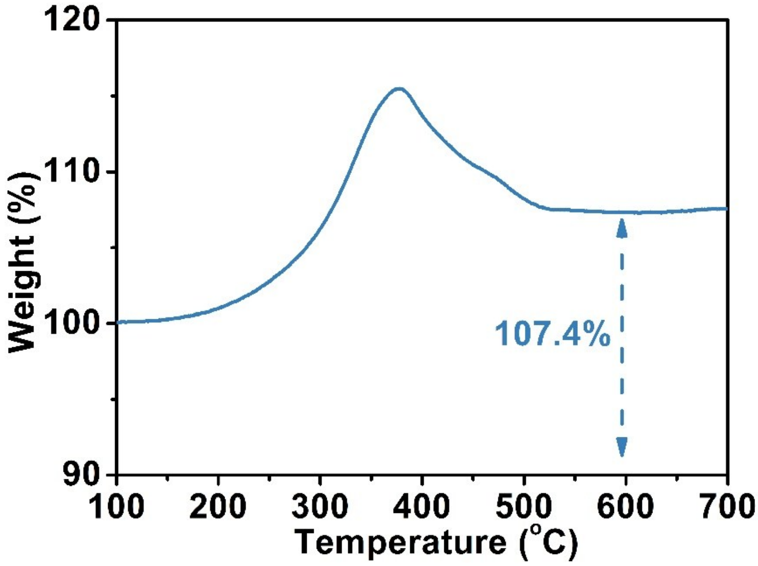

Fig. S2. TGA curve of MoO_2/MoC@C in O_2 with heating rate of 10 °C min^{-1}.

For TGA curve, the MoC and MoO_2 were gradually oxidated to MoO_3, with a weight loss of the combustion of carbon. Assuming that the sample is composed of stoichiometric MoC and carbon, and converts to only MoO_3 during the TGA measurement with remaining weight of ca. 107.4 wt%, the MoC content is estimated to be ca. 81.0 wt% in MoO_2/MoC@C according to the following equation:

$$M_{MoC} = 107.4 \text{ wt\%} * M_{MoC}/M_{MoO3} = 107.4 \text{ wt\%} * 108/144 \approx 81.0 \text{ wt\%}.$$

Assuming that the sample is composed of stoichiometric MoO_2 and carbon, and converts to only MoO_3 during the TGA measurement with remaining weight of ca. 107.4 wt%, the MoC content is estimated to be ca. 95.0 wt% in MoO_2/MoC@C according to the following equation:

$$M_{MoO2} = 107.4 \text{ wt\%} * M_{MoO2}/M_{MoO3} = 107.4 \text{ wt\%} * 128/144 \approx 95.0 \text{ wt\%}.$$

Namely, the content of carbon in MoO_2/MoC@C is estimated as 5~19 wt%.

Table S1. The amount of Mo, C and O in the composites detected by XPS analysis

Catalysts	Atomic (%)		
	Mo	C	O
MoO_2/MoC@C-750	15.46	47.06	37.49
MoO_2/MoC@C-850	11.57	67.83	20.60
MoO_2/MoC@C-950	3.66	88.93	7.41

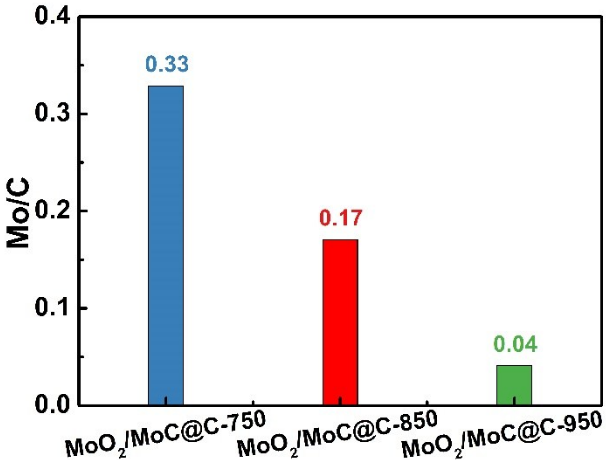

Fig. S3. Atomic ratio of Mo to C in MoO_2/MoC@C-750, MoO_2/MoC@C-850 and MoO_2/MoC@C-950.

Table S2. Fitting parameters (peak position, peak area and species percentage) for both Mo $3d_{5/2}$ and Mo $3d_{3/2}$ spectra taken on MoO_2/MoC@C-750, MoO_2/MoC@C-850 and MoO_2/MoC@C-950.

Samples	species		Peaks		Area		Mo-C/Mo-O
			$3d_{5/2}$	$3d_{3/2}$	$3d_{5/2}$	$3d_{3/2}$	($Mo_{carbide}/Mo_{oxide}$)
MoO_2/MoC @C-750	Mo-C	Mo^{3+}	229.1	232.2	500	335	0.02/0.98
	Mo-O	Mo^{4+}	229.9	233.0	6471	3463	
		Mo^{5+}	231.5	234.6	20600	13802	
		Mo^{6+}	233.1	236.2	5642	3780	
MoO_2/MoC @C-850	Mo-C	Mo^{2+}	228.5	231.6	2000	1340	0.3/0.7
		Mo^{3+}	229.1	232.2	24529	16434	
	Mo-O	Mo^{4+}	229.8	232.9	20644	13832	
		Mo^{5+}	232.1	235.2	33478	22430	
		Mo^{6+}	233.0	236.1	5553	3720	
MoO_2/MoC @C-950	Mo-C	Mo^{2+}	228.6	232.7	2030	1360	0.56/0.44
		Mo^{3+}	229.0	232.1	5094	3413	
	Mo-O	Mo^{4+}	229.8	232.9	3750	2512	
		Mo^{5+}	232.1	235.2	700	469	
		Mo^{6+}	233.0	236.1	1090	730	

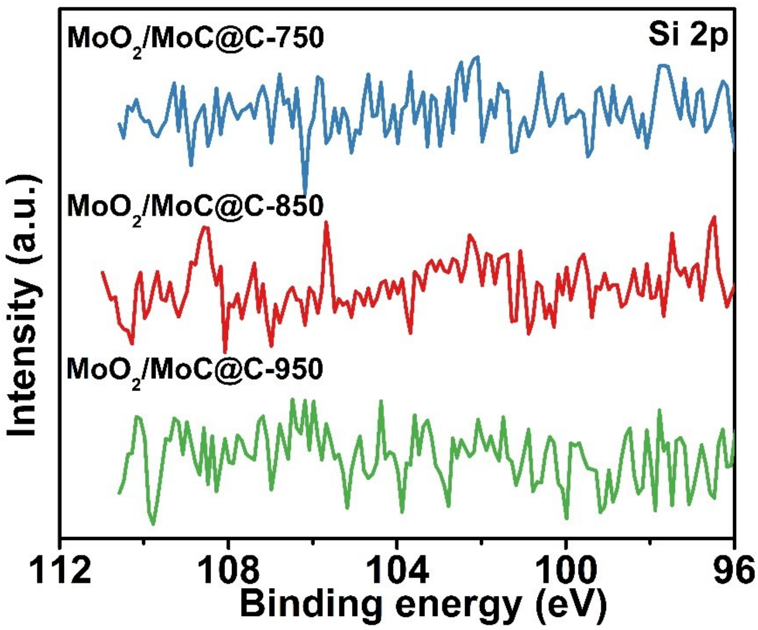

Fig. S4. XPS spectra of Si 2p in MoO_2/MoC@C-750, MoO_2/MoC@C-850 and MoO_2/MoC@C-950.

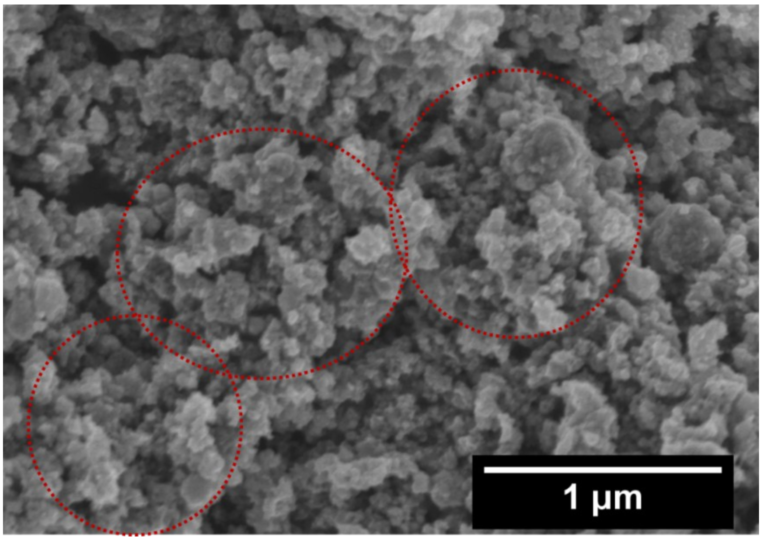

Fig. S5. SEM image of MoO_2/MoC@C-850.

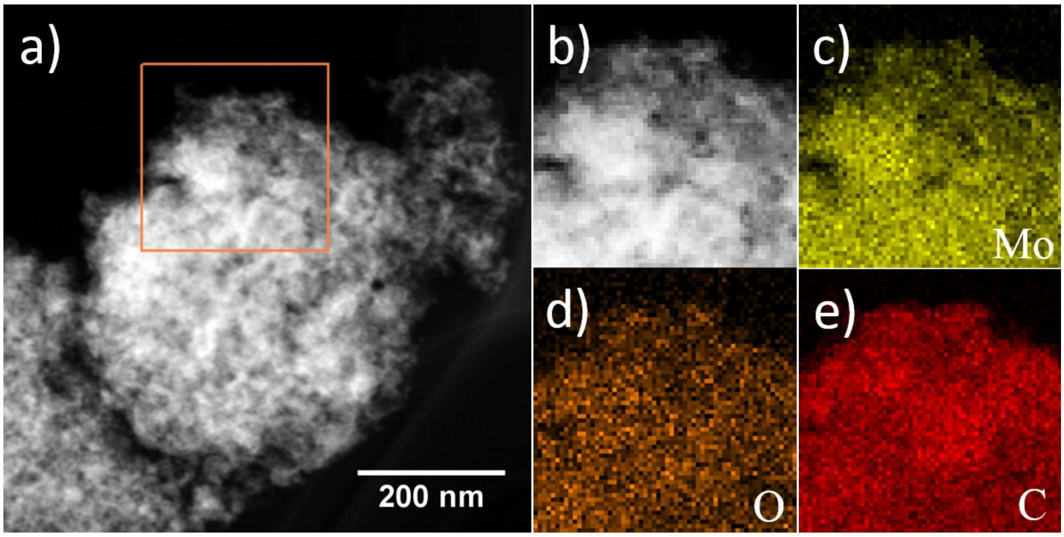

Fig. S6. (a, b) STEM images and EDX elemental mapping images of (c) Mo, (d) O, and (e) C elements.

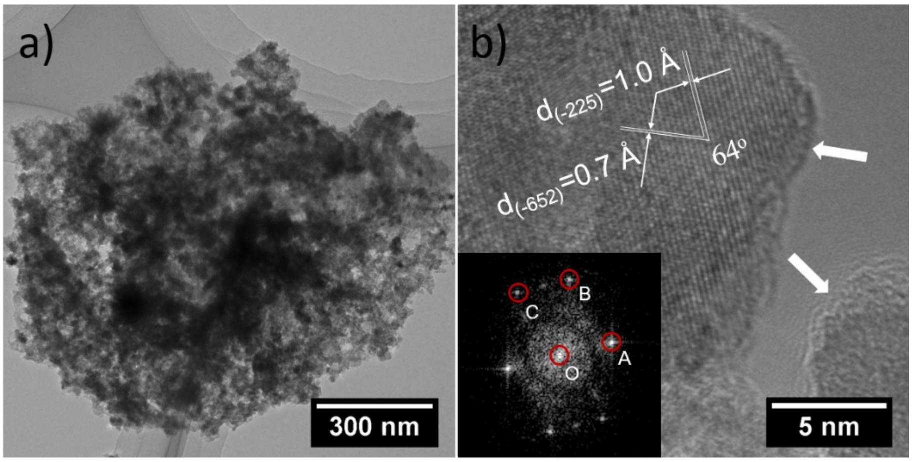

Fig. S7. (a) TEM and (b) HRTEM images of MoO_2/MoC@C-750.

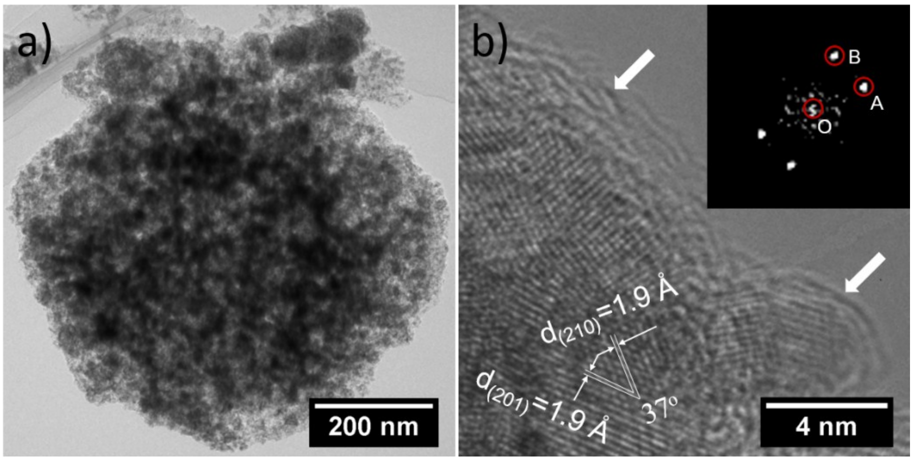

Fig. S8. (a) TEM and (b) HRTEM images of MoO_2/MoC@C-950.

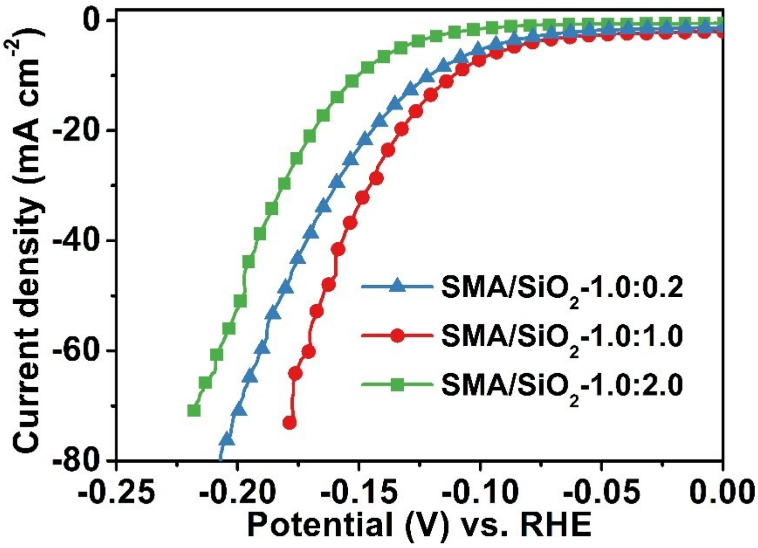

Fig. S9. Polarization curves of MoO_2/MoC@C-850 samples with different ratios of SMA/SiO_2. For clarification, the as-prepared samples were named SMA/SiO_2-X, which indicates the mass ratio (X) of SMA to SiO_2 in the synthesis. In the full paper, the samples of SMA/SiO_2-1.0:1.0 is also named as MoO_2/MoC@C-850.

Table S3. Key performance of representative Mo-based nanostructures.

Catalyst	Mass density (mg cm^{-2})	η_{20} (mV)	Tafel slope (mV/dec)	J_0 (mA cm^{-2})	J 100 mass activity[e] (mA cm^{-2} g^{-1})	Counter electrode	Electrolyte
Commercial Mo_2C particles[5]	1.4	225	56	1.3*10^{-3}	0.14	Pt	0.5 M H_2SO_4
Mo_2C/XC[6]	2	200(η_8)	59.4	8.1*10^{-3}	1.5	---	0.1 M HClO4
Mo_2C nanowires Mo_2C nanosheets[7]	0.357	220 260	55.8 64.5	---	2.8 2.8	Platinum wire	0.5 M H_2SO_4
Mo_2C/C-lamellas[8]	0.3	220	60.5	---	1.7	Platinum wire	0.5 M H_2SO_4
Mo_xC-G hybrids[9]	---	475(η_4)	115	---	--	Pt mesh	0.5 M H_2SO_4
$Mo_{2-x}Fe_xC$[10]	0.28	240 (η_5)	---	---	2.7	Graphite electrode	0.1 M $HClO_4$
MoWON/NGR[11]	0.212	270	84	---	37.7	Pt wire	0.5 M H_2SO_4
Co_6Mo_6C-G[12]	0.64	183	52	2.42*10^{-2}	6.25	A piece of graphite	0.5 M H_2SO_4
NiMo-NGTs[13]	2	79	67	0.84	13	Platinum foil	0.5 M H_2SO_4
$NiMo_2C$/NF[14]	---	47(η_{10})	36.8	0.51	--	Pt foil	6 M NaOH
Co-Mo_2C[15]	0.14	160 135	39 44	0.51 ---	17.9	Graphite electrode	0.5 M H_2SO_4 1M KOH
np-Mo_2C NWs[16]	0.21	150	53	---	14.3	Platinum foil	0.5 M H_2SO_4
Mo_2C@NPC/NPRGO[17]	0.14	50	33.6	1.9	285.7	Pt wire	0.5 M H_2SO_4
MoC-Mo_2C HNWs[18]	0.14	152 140	43 42	1.1*10^{-2}	28.6 30.7	Graphite electrode	0.5 M H_2SO_4 1M KOH
3DHP-Mo_2C[19]	0.28	125 140 110	60	0.28	42.9 40.4 60.7	---	0.5 M H_2SO_4 0.1M phosphate buffer 1M KOH
MoC_x nano-octahedrons[20]	0.8	160 175	53 59	0.023 ---	2.4 2.5	Graphite rod	0.5 M H_2SO_4 1M KOH
Mo_2C/C[21]	0.286	140 150	52 56	0.286	26.6 25.6	Graphite rod	0.5 M H_2SO_4 1M KOH
Mo_2C/C[22]	1	205	66.4	---	3	Platinum mesh	1M KOH
Mo_2C/WC NWs[23]	1.28	145	52	2.9*10^{-2}	0.4	Carbon rod	0.5 M H_2SO_4
Mo_2C@NC[24]	---	124(η_{10}) 156(η_{10}) 60(η_{10})	60	9.6*10^{-2} --- ---	-- -- --		0.5 M H_2SO_4 Neutral media 1M KOH
Mo_2C NPs@ carbon[25]	0.25	105	41	0.179	68	Pt plate	0.5 M H_2SO_4
β-Mo_2C nanotubes[26]	0.75	197 127	62 55	0.017 0.087	1.1 8.3	---	0.5 M H_2SO_4 0.1M KOH
Mo_2C/C[27]	0.213	180	55	0.047	0.94	Glassy	0.5 M H_2SO_4

						carbon	
Mo_2C nanorod[28]	0.43	175 180	58 45	0.033 0.011	4.7 14.0	Pt foil	0.5 M H_2SO_4 1M KOH
nanoMoC@GS[29]	1.02 0.76	150 90	43 50	0.0151 0.212	3.9 46.1	Graphite rod	0.5 M H_2SO_4 1M KOH
Ni-Mo_2C/C MF[30]	1	128	73	---	10.5	Platinum plate	1M KOH
Mo-$W_{18}O_{49}$[31]	0.8	75	54	0.5	>25	Pt	0.5 M H_2SO_4
NFL MoO_2/NF[32]	4.5	80	66	1.8	6.7	Graphite rod	1M KOH
MoO_2@PC-RGO[33]	0.14	90	41	0.48	>142.9	Pt wire	0.5 M H_2SO_4
Porous MoO_2/Ni foam[34]	3.4	40	41	---	>8.8	Graphite rod	1 M KOH
MoO_{3-x} [35]	0.2	170 240	56 72	---	20	Graphite rod	0.1 M KOH 0.1 M H_2SO_4
MoO_2/RGO/PI-CNT film[36]	0.04	170	68	---	250	Pt wire	0.5 M H_2SO_4
MoO_x/MoS_2[37]	0.273	320	63	---	0.4	Pt sheet	0.5 M H_2SO_4
MoS_2/MoO_2[38]	0.2	205	51	---	0.5	Graphite rod	0.5 M H_2SO_4
P doped MoO_{3-x}[39]	0.2	180 260	42 53	---	0.5 0.5	Platinum foil	0.5 M H_2SO_4 0.1 M KOH
MoO_3[40]	--	130(η_{10})	131	2.1	--	Pt wire	1 M H_2SO_4
MoO_2/MoC@C This work	0.57	133 203	77.3 104.7	0.371 0.267	12.5 4.1	Graphite rod	0.5 M H_2SO_4 1 M KOH

[a] η_{20}: Overpotential required to drive a current density of 20 mA cm^{-2}. [b] J_0: Exchange current density. [c] η_{10}: Overpotential required to drive a current density of 10 mA cm^{-2}. [d] η_8: Overpotential required to drive a current density of 8 mA cm^{-2}. [e] η_5: Overpotential required to drive a current density of 5 mA cm^{-2}. [f] η_4: Overpotential required to drive a current density of 4 mA cm^{-2}. [g] J 100 mass activity: Current density according to the loading mass of catalysts at overpotential of 100 mV. J 100 mass activity=j/m, where j is the current density and m is the loading mass of catalysts on the electrode.

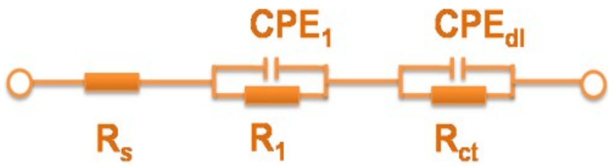

Fig. S10. Equivalent circuit used to fit the EIS data. R_s is the overall series resistance, CPE_1 and R_1 are the constant phase element and resistance describing electron transport at GCE/electrocatalyst interface, respectively, CPE_{dl} is the constant phase element of the electrocatalyst/electrolyte interface, and R_{ct} is the charge transfer resistance at electrocatalyst /electrolyte interface.

Table S4. The fitting results of EIS spectra in acid solution

Sample	R_s (Ω)	Q_1 (F cm^{-2} S^{n-1})	n_1	R_1 (Ω)	Q_{ct} (F cm^{-2} S^{n-1})	n_{ct}	R_{ct} (Ω)
MoO_2@C-750	7.0	7.649 e-4	0.7086	17.6	8.172 e-3	0.2617	167.4
MoO_2@C-850	8.4	2.024e-3	0.7617	2.3	6.523e-3	0.4605	25.8
MoO_2@C-950	7.7	7.333e-4	0.7022	14.1	9.027e-4	0.3874	120.8

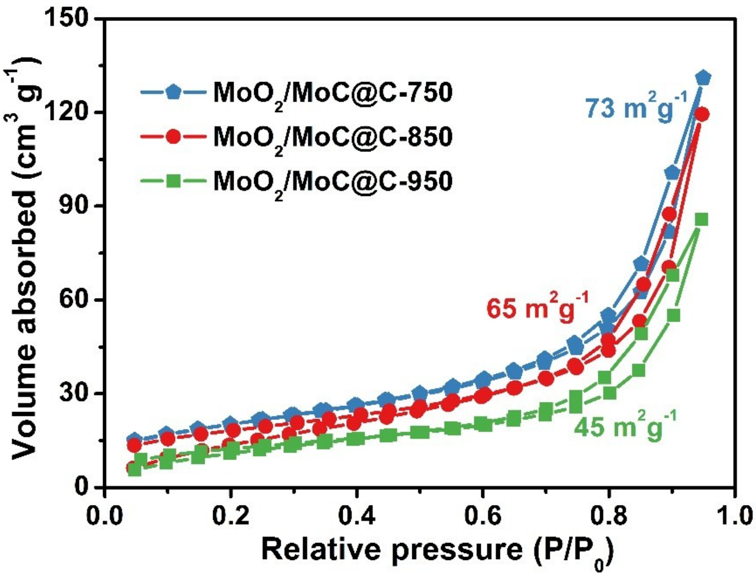

Fig. S11. Nitrogen adsorption/desorption isotherm of MoO_2/MoC@C-750, MoO_2/MoC@C-850 and MoO_2/MoC@C-950.

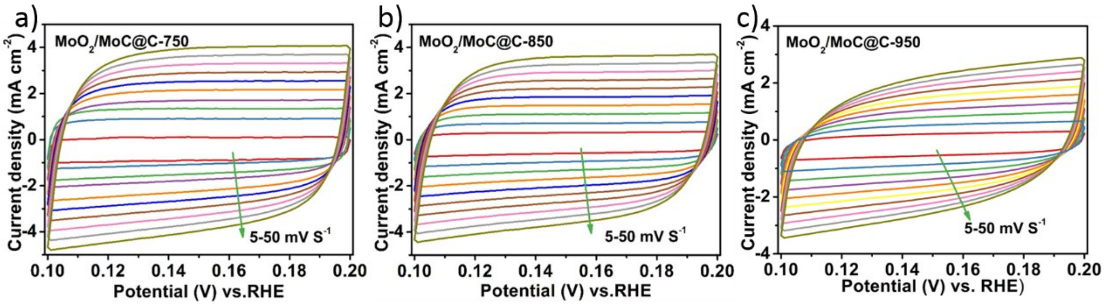

Fig. S12. Cyclic voltammograms in the region of 0.1-0.2 V vs. RHE for the (a) MoO_2/MoC@C-750, (b) MoO_2/MoC@C-850, and (c) MoO_2/MoC@C-950.

Table S5. Surface energy of MoO_2.

Crystal face	Surface energy (eV/Å^2)
(001)	0.20
(010)	0.20
(100)	0.19
(101)	0.14
(110)	0.16
(011)	0.18
(111)	0.16

Table S6. Surface energy of MoC.

Crystal face	Surface energy (eV/Å^2)
(001)	0.14
(011)	0.19
(111)	0.20

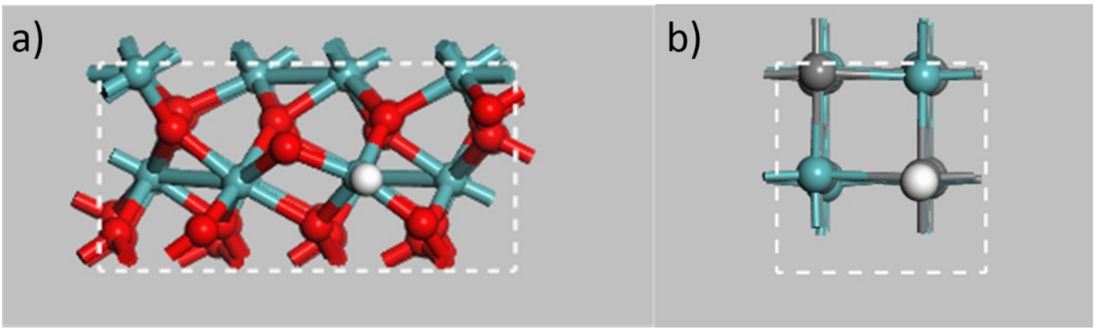

Fig. S13. Optimized structures of H* adsorbed on the surface of (a) MoO_2 (101) plane and (b) MoC (001) plane. Cyan balls denote molybdenum atoms, red ones denote oxygen atoms, gray ones denote carbon atoms, and white ones denote hydrogen atoms.

Reference

1. S. J. Clark, M. D. Segall, C. J. Pickard, P. J. Hasnip, M. J. Probert, K. Refson and M. C. Payne, *Z. Kristallogr.*, 2005, **220**, 567-570.
2. G. Kresse and J. Hafner, *J. Phys. Cond. Matter*, 1994, **6**, 8245-8257.
3. J. P. Perdew, K. Burke and M. Ernzerhof, *Phys. Rev. Lett.*, 1996, **77**, 3865-3868.
4. P. Jiang, Y. Yang, R. Shi, G. Xia, J. Chen, J. Su and Q. Chen, *J. Mater. Chem. A*, 2017, **5**, 5475-5485
5. H. Vrubel and X. Hu, *Angew. Chem. Int. Ed.* , 2012, **51**, 12703-12706.
6. W. F. Chen, C. H. Wang, K. Sasaki, N. Marinkovic, W. Xu, J. T. Muckerman, Y. Zhu and R. R. Adzic, *Energy Environ. Sci.*, 2013, **6**, 943-951.
7. C. Ge, P. Jiang, W. Cui, Z. Pu, Z. Xing, A. M. Asiri, A. Y. Obaid, X. Sun and J. Tian, *Electrochim. Acta*, 2014, **134**, 182-186.
8. L. Peng, Y. Nie, L. Zhang, R. Xiang, J. Wang, H. Chen, K. Chen and Z. Wei, *ChemCatChem*, 2017, **9**, 1588-1593.
9. J. Wu, L. Ma, A. Samanta, M. Liu, B. Li, Y. Yang, J. Yuan, J. Zhang, Y. Gong, J. Lou, R. Vajtai, B. Yakobson, A. K. Singh, C. S. Tiwary and P. M. Ajayan, *Adv. Mater. Interfaces*, 2017, **4**, 1600866-1600871.
10. C. Wan and B. M. Leonard, *Chem. Mater.*, 2015, **27**, 4281-4288.
11. A. C. Mtukula, X. Bo and L. Guo, *J. Alloy. Compd.*, 2017, **692**, 614-621.
12. C. He and J. Tao, *J. Catal.*, 2017, **347**, 63-71.
13. T. Wang, Y. Guo, Z. Zhou, X. Chang, J. Zheng and X. Li, *ACS Nano*, 2016, **10**, 10397-10403.
14. K. Xiong, L. Li, L. Zhang, W. Ding, L. Peng, Y. Wang, S. Chen, S. Tan and Z. Wei, *J. Mater. Chem. A*, 2015, **3**, 1863-1867.
15. H. Lin, N. Liu, Z. Shi, Y. Guo, Y. Tang and Q. Gao, *Adv. Funct. Mater.*, 2016, **26**, 5590-5598.
16. L. Liao, S. Wang, J. Xiao, X. Bian, Y. Zhang, M. D. Scanlon, X. Hu, Y. Tang, B. Liu and H. H. Girault, *Energy Environ. Sci.*, 2014, **7**, 387-392.
17. J. Li, Y. Wang, C. Liu, S. Li, Y. Wang, L. Dong, Z. Dai, Y. Li and Y. Lan, *Nat. Commun.*, 2016, **7**, 11204-11211.
18. H. Lin, Z. Shi, S. He, X. Yu, S. Wang, Q. Gao and Y. Tang, *Chem. Sci.*, 2016, **7**, 3399-3405.
19. H. Ang, H. Wang, B. Li, Y. Zong, X. Wang and Q. Yan, *Small*, 2016, **12**, 2859-2865.
20. H. Wu, B. Xia, L. Yu, X. Yu and X. Lou, *Nat. Commun.*, 2015, **6**, 6512-6519.
21. Y. Mu, Y. Zhang, L. Fang, L. Liu, H. Zhang and Y. Wang, *Electrochim. Acta*, 2016, **215**, 357-365.
22. M. Qamar, A. Adam, B. Merzougui, A. Helal, O. Abdulhamid and M. N. Siddiqui, *J. Mater. Chem. A*, 2016, **4**, 16225-16232.
23. P. Xiao, X. Ge, H. Wang, Z. Liu, A. Fisher and X. Wang, *Adv. Funct. Mater.*, 2015, **25**, 1520-1526.
24. Y. Liu, G. Yu, G. Li, Y. Sun, T. Asefa, W. Chen and X. Zou, *Angew. Chem. Int. Ed.*, 2015, **54**, 10752-10757.
25. R. Ma, Y. Zhou, Y. Chen, P. Li, Q. Liu and J. Wang, *Angew. Chem. Int. Ed.*,

2015, **54**, 14723-14727.
26. F. Ma, H. Wu, B. Xia, C. Xu and X. Lou, *Angew. Chem. Int. Ed.*, 2015, **54**, 15395-15399.
27. C. Tang, Z. Wu and D. Wang, *ChemCatChem*, 2016, **8**, 1961-1967.
28. P. Xiao, Y. Yan, X. Ge, Z. Liu, J.-Y. Wang and X. Wang, *Appl. Catal. B-Environ.*, 2014, **154-155**, 232-237.
29. Z. Shi, Y. Wang, H. Lin, H. Zhang, M. Shen, S. Xie, Y. Zhang, Q. Gao and Y. Tang, *J. Mater. Chem. A*, 2016, **4**, 6006-6013.
30. L. Sun, C. Wang, Q. Sun, Y. Cheng and L. Wang, *Chem. Eur. J.*, 2017, **23**, 4644-4650.
31. X. Zhong, Y. Sun, X. Chen, G. Zhuang, X. Li and J. Wang, *Adv. Funct. Mater.*, 2016, **26**, 5778-5786.
32. Y. Jin and P. K. Shen, *J. Mater. Chem. A*, 2015, **3**, 20080-20085.
33. Y. Tang, M. Gao, C. Liu, S. Li, H. Jiang, Y. Lan, M. Han and S. Yu, *Angew. Chem. Int. Ed.*, 2015, **54**, 12928-12932.
34. Y. Jin, H. Wang, J. Li, X. Yue, Y. Han, P. Shen and Y. Cui, *Adv. Mater.*, 2016, **28**, 3785-3790.
35. Z. Luo, R. Miao, T. D. Huan, I. M. Mosa, A. S. Poyraz, W. Zhong, J. E. Cloud, D. A. Kriz, S. Thanneeru, J. He, Y. Zhang, R. Ramprasad and S. L. Suib, *Adv. Energy Mater.*, 2016, **6**, 1600528-1600538.
36. X. Li, Y. Jiang, L. Jia and C. Wang, *J. Power Source*, 2016, **304**, 146-154.
37. B. Jin, X. Zhou, L. Huang, M. Licklederer, M. Yang and P. Schmuki, *Angew. Chem. Int. Ed.* , 2016, **55**, 12252 -12256.
38. J. Wang, W. Wang, Z. Wang, J. G. Chen and C. Liu, *ACS Catal.*, 2017, **6**, 6585-6590.
39. L. Li, T. Zhang, J. Yan, X. Cai and S. Liu, *Small*, 2017, **13**, 1700441-1700447.
40. H. Sinaim, D. J. Ham, J. S. Lee, A. Phuruangrat, S. Thongtem and T. Thongtem, *J. Alloy. Compd.*, 2012, **516**, 172-178.